



36 deposition caused by transport between neighbouring regions (i.e. Europe and Russia) occurs
37 throughout the whole year (slightly stronger in winter), while that by transport over long
38 distances (i.e. from East Asia to North America) mainly takes place in spring and fall, which is
39 consistent with the seasonality found for hemispheric transport of air pollutants. Deposition in
40 emission intense regions such as East Asia is dominated (~80%) by own region emission, while
41 deposition in low emission regions such as Russia is almost equally affected by own region
42 emission (~40%) and foreign impact (~23-45%). We also find that deposition on the coastal
43 regions or near coastal open ocean is twice more sensitive to hemispheric transport than non-
44 coastal continental regions, especially for regions (i.e. west coast of North America) in the
45 downwind location of major emission source regions. This study highlights the significant
46 impact of hemispheric transport on deposition in coastal regions, open ocean and low emission
47 regions. Further research is proposed for improving ecosystem and human health in these
48 regions, with regards to the enhanced hemispheric transport.

49 **1 Introduction**

50 The increasing consumption of energy by human activities has largely increased the deposition
51 of sulfur (S) and nitrogen (N) over the terrestrial and marine ecosystem in recent years (Kim et
52 al., 2011; Galloway et al., 2008; Duce et al., 2008) and the amount of atmospheric deposition is
53 estimated to continue increasing in the near future (Bleeker et al., 2011; Lamarque et al., 2013;
54 Kanakidou et al., 2016; Paulot et al., 2013; Lamarque et al., 2005). While deposition supplies
55 ecosystem with nutrients, too much deposition could cause various adverse impacts on the
56 environment, including acidification and eutrophication of the forest and waterbody (Bouwman
57 et al., 2002; Bergstrom and Jansson, 2006; Dentener et al., 2006; Phoenix et al., 2006), soil
58 acidification that slows down the crop production (Guo et al., 2010; Janssens et al., 2010) and
59 even decrease plant biodiversity (Bobbink et al., 2010; Clark and Tilman, 2008). The control of
60 deposition has become a growing worldwide concern.

61 Hemispheric transport of air pollutants is found to aggravate the regional air pollution
62 (Wild and Akimoto, 2001; Sudo and Akimoto, 2007; Fu et al., 2012; Fiore et al., 2009) as well as
63 enlarge the local deposition burden (Glotfelty et al., 2014; Sanderson et al., 2008). Air pollution
64 from Asia contributes to the concentration of PM_{2.5} in western United States by 1.5 µg m⁻³ (Tao
65 et al., 2016), the O₃ concentration by 3-10 ppbv (Zhang et al., 2009; Zhang et al., 2008; Yienger



66 et al., 2000; Reidmiller et al., 2009; Jacob et al., 1999; Brown-Steiner and Hess, 2011) and the
67 peroxyacyl nitrate (PAN) concentration by 26 ppbv (Berntsen et al., 1999) in spring. The long-
68 range transport of air pollution from North America is estimated to contribute by 3-5 ppb to (7-
69 11%) to the O₃ concentration in Europe annually (Auvray and Bey, 2005; Guerova et al., 2006;
70 Derwent et al., 2004; Li et al., 2002) and the increment can reach 25-28 ppbv during particular
71 events (Guerova et al., 2006). European outflow affects the surface O₃ concentration in western
72 China by 2-6 ppbv in spring and summer (Li et al., 2014) and North Africa by 5-20 ppbv in
73 summer (Duncan et al., 2008; Duncan and Bey, 2004). The study by Yu et al. (2013) found that
74 the long-range transport contributes by 6-16% and 22-40% to aerosol optical depth and direct
75 radiative forcing in 4 regions including North America, Europe, East Asia and South Asia.
76 Recent studies have reported an increasing trend in the hemispheric transport of air pollution. In
77 particular, the air pollution exported from Asia to North America has increased significantly in
78 recent years (Jaffe et al., 2003; Parrish et al., 2009; Parrish et al., 2004; Verstraeten et al., 2015;
79 Zhang et al., 2008) due to the rapid growth of Asian emission (Richter et al., 2005; Lu et al.,
80 2010; Zhang et al., 2007; van der A et al., 2006; van der A et al., 2008).

81 Compared to the impact on air pollution, the impact of hemispheric transport on
82 deposition hasn't been fully studied. Arndt and Carmichael (1995) developed a source-receptor
83 (S-R) relationship for S deposition among the Asia regions in early 1900s. Zhang et al. (2012)
84 found foreign anthropogenic emission contributes to 6% and 8% of the NO_y and NH_x deposition
85 in contiguous United States, respectively. A systematic study by Sanderson et al. (2008) shed
86 light on the impact of long-range transport on deposition of oxidized nitrogen at global scale.
87 That study uses the model ensemble results from phase I of Task Force Hemispheric Transport
88 of Air Pollution (HTAP I) to calculate the S-R relationship for NO_y deposition in 2001 among 4
89 regions: Europe, North America, South Asia and East Asia. Results showed that about 12-24%
90 of the NO_x emission is deposited out of source regions. About 3-10% of the emission is
91 deposited on the other 3 regions and affects their deposition by about 1-3%. However, these
92 studies focused on emission intense regions, where the foreign disturbance is relatively small
93 compared to huge own region emission. The foreign impact on low emission regions was not
94 evaluated in the same detail. Furthermore, both the magnitude and spatial distribution of S and N
95 emission and deposition have been changed considerably during the last 10 years (2001-2010)



96 (Tan et al., 2018). It is necessary to update the S-R relationship for more recent years with
97 regards to these changes.

98 To explore these questions, this study assesses the impact of hemispheric transport of S,
99 NO_x and NH₃ emissions on S and N deposition, with multi-model ensemble results from 2nd
100 phase of HTAP (HTAP II). Additional to the 4 regions: North America (NA), Europe (EU),
101 South Asia (SA), East Asia (EA) used in Sanderson's (2008) study for HTAP I, we include 2
102 regions: Middle East (ME) and Russia, Belarussia, Ukraine (RU) in this study. These two
103 regions have low S and N emissions relative to their areal extent, but are located close to high
104 emission regions such as EU, SA and EA. We calculate the amount of deposition brought by
105 hemispheric transport by comparing model results for base case and for 20% emission
106 perturbation cases. The experimental design is described in Section 2. Section 3 is the result part
107 and has 3 subsections. We explore the following questions:

- 108 1) Which fraction (percentage) of the S or N emissions is transported and deposited outside of
109 this region? Which fraction is finally deposited on the other 5 receptor regions, other regions
110 and oceans? What is the seasonality of the exported fraction?
- 111 2) As receptor regions, what is the amount of deposition brought by hemispheric transport?
112 How much will it affect the local deposition? Is there any seasonality for this impact?
- 113 3) For each region, what are the contributions of hemispheric transport from foreign regions and
114 of control of own region emission on deposition? In line with the analysis for other pollutants,
115 to this purpose we evaluate the so-called response to extra-regional emission reduction
116 (RERER) metric. We also discuss the own region and foreign impact specifically on the
117 coastal regions. The inter-model variations are also illustrated in this section.

118 Section 4 is a summary of the findings in this study and some suggestions for future study.

119 **2 Methodology**

120 **2.1 HTAP II and experiment set-up**

121 The HTAP was created in 2004 under the Convention on Long-range Transboundary Air
122 Pollution (CLRTAP). The project involves efforts from international scientists aiming at
123 understanding the hemispheric transport of air pollutants and its impact on regional and global
124 air quality, public health and near-term climate change. Until now, two phases of HTAP
125 experiments have been conducted successfully. The HTAP I involved more than 20 models from



126 international modelling groups, with 2001 as the base year for modeling studies. A
127 comprehensive report of the major findings of HTAP was released in 2010 and could be
128 downloaded from <http://www.htap.org/>. The HTAP II was launched in 2012, with 2010 as the
129 base simulation year. HTAP II required all models to use the same prescribed anthropogenic
130 emission inventory and boundary conditions instead of using the best estimates of emission by
131 each model group as HTAP I, which facilitated an inter-model comparison between models. In
132 addition, HTAP II had a refined definition for the boundaries of regions, which enabled an
133 update in the S-R relationships for air pollutants and deposition among regions.

134 This study uses the ensemble of 11 global models from HTAP II (including CAM-Chem,
135 CHASER_re1, CHASER_t106, EMEP_rv48, GEMMACH, GEOS5, GEOSCHEMAJOINT,
136 OsloCTM3v.2, GOCARTv5, SPRINTARS and C-IFS_v2). A detailed description of the
137 experiment set-up could be found in Galmarini et al. (2017). The S deposition includes SO₂
138 deposition and SO₄²⁻ deposition. N deposition is categorized to oxidized nitrogen (NO_y) and
139 reduced nitrogen (NH_x) deposition. NO_y deposition is a sum of all oxidized N except N₂O,
140 including NO₂, HNO₃, NO₃⁻, PAN and other organic nitrates than PAN (Orgn). NH_x deposition
141 includes NH₃ deposition and NH₄⁺ deposition. To form the multi-model ensemble, we re-grid all
142 models to a uniformed horizontal resolution of 0.1° × 0.1°. We use the multi-model mean value
143 (MMM) of all models to present the ensemble results, a procedure which has previously been
144 proven to have a better agreement with observations than single model results (Dentener et al.,
145 2006; Tan et al., 2018). The mean values of the compositions of S or N deposition are calculated
146 separately and then are combined to compute the total S or N deposition. More details can be
147 found in Tan et al. (2018). The inter-model variations are discussed in section 3.3.

148 2.2 Simulation scenarios

149 The base simulation uses anthropogenic emissions in 2010 (Janssens-Maenhout et al.,
150 2015), which is called “base case” in this study. The MMM performance on wet deposition has
151 been evaluated with observations from National Atmospheric Deposition Program (NADP)
152 (<http://nadp.sws.uiuc.edu/>) for NA, European Monitoring and Evaluation Programme (EMEP)
153 CCC reports (<http://www.nilu.no/projects/ccc/reports.html>) for EU and Acid Deposition
154 Monitoring Network in East Asia (EANET) (<http://www.eanet.asia/>) for EA in Tan et al. (2018).
155 In terms of wet deposition, MMM results are evaluated with site observation of deposition. SO₄²⁻



156 wet deposition is generally well simulated with 76% of the stations of all networks predicted
157 within $\pm 50\%$ of observation. Negative model biases (-20%) are found at some East Asian
158 stations. Modeled NO_3^- wet deposition is within $\pm 50\%$ of observation for 83% of the stations of
159 all networks. The European and Southeast Asian stations with high observed NO_3^- wet deposition
160 are found to be somewhat underestimated. 81% of modeled NH_4^+ wet deposition at stations of all
161 networks are within $\pm 50\%$ of observation. A general underestimation is found in modelled NH_4^+
162 wet deposition, especially at East Asian stations. In terms of dry deposition, due to the lack of
163 directly measured dry deposition, we compare the modeled dry deposition with inferential data
164 from the Clean Air Status and Trends Network (CASTNET) over United States. The CASTNET
165 inferential data is calculated with observed aerosol concentration and modelled dry deposition
166 velocity, therefore it has high uncertainty in data quality. Results show that the modelled dry
167 deposition is generally a factor of 1-2 higher than the CASTNET inferential data. This is a
168 common feature of many global and regional models (WMO, 2017) and subject to further
169 research.

170 In addition to the base case simulations, emission perturbation experiments are conducted
171 for certain regions. The boundaries of 17 regions in HTAP II are defined in Fig. 1. In the
172 perturbation experiments, the anthropogenic emissions (including NO_x , SO_2 , NH_3 , VOC, CO
173 and PM) of specific regions (i.e. NA) are reduced by 20% from the amounts in the base case
174 simulation, while the other regions keep the same emissions. This study uses the perturbation
175 experiments of 6 regions (with color in Fig.1) with high priority: NA, EU, SA, EA, ME and RU.
176 In addition, a global perturbation experiment referred as “GLO” is conducted with 20% decrease
177 in global anthropogenic emissions. We estimate the impact of hemispheric transport on
178 deposition by comparing the model results under perturbation experiments with those under base
179 case simulation. In order to validate the quality of model outputs, we check the mass balance
180 between emission and deposition at global scale. The mass balance for base case simulation has
181 been checked in Tan et al. (2018), therefore we show the mass balance for perturbation
182 experiments in this study. We compare the global total amounts of changes of deposition (Δ
183 Depo) with changes of emissions (Δ Emis) for all perturbation cases (Table S1). According to
184 our results, the amounts of Δ Depo are almost identical to Δ Emis for all perturbation cases. The
185 Δ Depo of NH_x deposition under EA perturbation case is not available due to that no model
186 meets the mass balance requirements mentioned above.



187 3 Results

188 3.1 Export of S and N emissions from source regions

189 This section studies the export of S and N emissions and oxidation products from source regions.
190 Table 1 shows the S-R relationship of S and N deposition among the 6 regions. The numbers are
191 the sensitivity ($SEN_{r \rightarrow s}$) of deposition in the receptor/source regions to emission changes in the
192 source regions (Sanderson et al., 2008). The metric is calculated as Δ Depo in the receptor/source
193 regions divided by Δ Emis in the source regions following equation (1).

$$194 \quad SEN_{r \rightarrow s} = \frac{\Delta Depo (r/s)}{\Delta Emis (s)} \times 100\% \quad (1)$$

195 where s is the source region and r is the receptor region. Δ Depo (r/s) is the deposition change in
196 the receptor/source regions, Δ Emis (S) is the emission change in the source regions. This value
197 indicates the fraction of emission from source regions that is deposited locally or exported to
198 foreign regions.

199 The numbers in Table 1 are for coastal and non-coastal regions together and the numbers
200 in the parenthesis are specifically for coastal regions (defined in Fig. 1). “Others” means the
201 other regions in the world than the 6 regions (white color in Fig. 1). The NA region has 69% of
202 its S emission deposited within itself, including 9% deposited on its coastal region. The
203 remaining 31% is exported to the other regions, mostly to the “Others” and less than 1% is
204 deposited on the other 5 regions (EU, SA, EA, ME and RU). A relatively large fraction (14 %) of
205 European S emissions are exported to RU region. Other major pathways of export of sulphur
206 emissions/reaction products are from SA to EA (9%), from EA to RU (5%) and from RU to EU
207 (7%) and EA (5%). ME has considerable percentages of S emission exported to its nearby
208 regions such as SA (8%), EA (5%) and RU (5%). The S-R relationship of NO_y deposition is
209 similar to that of S deposition, except that EU and ME have 66% and 54% of NO_x emissions
210 deposited within the source region, which are 6% and 12% higher than those of S emissions,
211 likely due to the large average emission altitude of S emissions and somewhat longer lifetimes
212 compared to NO_x emissions. In terms of NH_x deposition, about 20% more NH_3 emission is
213 deposited within the source region due to its short lifetime in the atmosphere.

214 The seasonal variation of the export of S and N emissions by source regions is shown in
215 Fig. S1. In terms of S emission, there is 5-10% of seasonal variation around the annual average



216 of 25% in the export fractions for all regions except SA. SA exports almost half of its annual S
217 emission in spring, which is twice the numbers in summer (20%) and fall (25%), related to the
218 specific dry period and monsoon circulation. The seasonal export fractions of NO_x and NH_3
219 emission are similar to that of S emission, but generally lower in all seasons. Generally, the
220 source regions export highest percentage of their emissions in winter and spring and lowest in
221 summer. More proficient oxidation chemistry in summer resulting in more soluble component,
222 and local weather systems, especially the episodic of precipitation has large influence on this
223 seasonality. For most continental regions, the wet deposition accounts for 50-70% of total
224 deposition (Tan et al., 2018; Vet et al., 2014; Dentener et al., 2006). Therefore, local
225 precipitation washes out large proportion of the air pollutants in the atmosphere during the
226 rainfall seasons (i.e. summer). In addition, the strong westerly winds in winter and spring favor
227 the hemispheric transport, while the rapid vertical convection in summer slows down the zonal
228 transport of air flows and accelerates the removal process.

229 We compare our results with previous studies. Bey et al. (2001) estimated that 70% of
230 emitted NO_x from Asia is lost within its boundary by deposition of HNO_3 in spring. The
231 estimation in our study is 70% for EA and 61% for SA, close to Bey's result. Li et al. (2004)
232 reported that about 20% of anthropogenic NO_x emitted by NA is deposited out of its boundary
233 (about 1000 km offshore). Stohl et al. (2002) calculated that 9-22% of surface NO_y emissions is
234 exported out of the boundary layer of NA. Our result is about 30%, higher than Li's and Stohl's
235 results. HTAP I study by Sanderson et al. (2008) developed a SR relationship for NO_y deposition
236 among NA, EU, SA and EA. About 12-24% of the emitted NO_x is deposited out of source
237 regions and the corresponding percentage in this study is 26-34%. It should be noted that the
238 estimations of different studies are influenced by several factors and the results are not fully
239 comparable. (1) Definition of boundaries of source and receptor regions. For instance, Li et al.
240 (2004) defined the boundary of NA by a squared domain: 65-130°W, 25-55°N, while we use the
241 continental boundaries defined by HTAP II. There are also changes in the definition of
242 boundaries between HTAP II and HTAP I. For instance, HTAP I includes Mexico and Central
243 America in NA, but they are defined as a separate region in HTAP II (region 12 in Fig. 1). The
244 boundary of EU is also changed in HTAP II. (2) HTAP I used the perturbation simulation that
245 only reduce the NO_x emission, but HTAP II simulations also reduce other anthropogenic



246 emissions, including SO₂ and PM. The joint control of multiple emissions may cause more
247 reduction in NO_y deposition and it is hard to estimate this effect in this study.

248 3.2 Impact of hemispheric transport on deposition

249 This section investigates the impact of hemispheric transport on deposition in the receptor
250 regions. Fig. 2 is annual response of S deposition to 20% emission reduction in source regions,
251 calculated as (Δ Depo under perturbation case) / (deposition in base case) \times 100%. The negative
252 values mean that the corresponding deposition decreases with reduction in emission. Table S2
253 summarizes the regional median deposition fluxes under base case and under emission
254 perturbation in source regions. Fig. 2(a) shows the global response of deposition to 20%
255 emission reduction in NA. The largest changes happen in the source region NA, with a 5-20%
256 decrease in S deposition in the non-coastal region and 15-20% decrease at the east coast. The
257 impact on the North Atlantic Ocean deposition declines gradually from near coastal region (12-
258 15%) to open ocean (5-12%) and Eurasia (<1%). Fig. 2(b) shows the global response of
259 deposition to 20% emission reduction in EU. Although the impact on continental non-coastal
260 regions is high (12-20%), the impact on the coastal regions is within 5%, much lower than NA's
261 impact on its east coast (15-20%). The deposition in North Africa, central Asia and western RU
262 is affected by 2-5%. 20% emission reduction in SA (Fig. 2(c)) shows large influence over its
263 south-west coast and the Arabian Sea (5-12%). The SA's outflow affects the deposition in
264 southeastern ME and eastern Sub Saharan Africa by 1-5% and western EA and Southeast Asia
265 (Bangladesh) by 2-10%. Fig. 2(d) shows the impact of 20% emission reduction on deposition in
266 EA. On one hand, the impact is strong on the east coast of China (12-15%) and decreases
267 gradually over the North Pacific Ocean (5-15%). Although the majority of S emission is
268 deposited on the Pacific Ocean, the influence on western NA can still reach 5-8%. On the other
269 hand, the impact on Southeast Asia and South Asia is much lower (2-5% and <1%), due to the
270 block of air flows by the Himalaya Mountains (Fig. S4). 20% emission decrease in ME mainly
271 affects the S deposition in Africa by 2-10% and western EA by 2-5%. Fig. 2(f) shows the S
272 deposition change with 20% emission reduction in RU. The regions of impact are mainly at high
273 latitudes, including northern EU (2-5%) and western Arctic Circle (1-5%).

274 The impact of NO_x emission reduction on NO_y deposition from each source region is
275 shown in Fig 3. The overall impact is qualitatively similar to that of S emission with some



276 differences. For some regions, the impact of hemispheric transport on NO_y deposition is lower
277 than that on S deposition. For instance, SA's impact on eastern Africa is about 2-5% on S
278 deposition, but is <1% on NO_y deposition. ME's impact on the east coast of Africa and Gulf of
279 Guinea is about 2-5% on S deposition, but is <1% on NO_y deposition. These smaller sensitivities
280 reflect differences in lifetimes, and the lower formation of aerosol nitrate under warm conditions
281 in tropical regions. Under the NA perturbation case (Fig. 3(a)), a 2-12% change of NO_y
282 deposition is found on the west coast of California, due to high NO_x emission in California from
283 mobile source, which is not seen in S deposition. The impact of emission reduction in EU and
284 EA on their coastal regions is generally 2-5% higher for NO_y deposition than S deposition (Fig.
285 3(b) and (d)). The impact on NH_x deposition is similar to NO_y deposition (Fig. S2). It should be
286 noted that this is the result from 20% emission reduction in the source regions, therefore the
287 actual impact (100% emission reduction) could be 5 times higher when assuming a linear
288 relationship between 20 and 100% emission reduction on deposition.

289 We quantify the amount of deposition carried by hemispheric transport and study its
290 seasonality. Fig. 4 shows the monthly changes of S deposition for 20% emission reductions in
291 source regions. The values are meridional sum with a west-east resolution of 0.1 degree, and
292 display well the locations of the source regions. The negative values indicate the amounts of
293 pollutants transported from source regions to receptor regions. According to Fig 4(a), NA has
294 about $(1-10) \times 10^4 \text{ kg(S) month}^{-1}$ per 0.1° longitude of its S emission transported and deposited
295 over the North Atlantic Ocean (15-75°W) throughout the whole year. We also find about $(1-3)$
296 $\times 10^4 \text{ kg(S) month}^{-1}$ per 0.1° longitude decrease of S deposition at about 90°E and 120°E in
297 spring and fall, which gives evidence to NA's influence on Eurasia via transatlantic flow,
298 although this amount accounts for less than 1% of local S deposition (white in Eurasia in
299 Fig.2(a)). Fig. 4(b) shows that about $(1-3) \times 10^4 \text{ kg(S) month}^{-1}$ per 0.1° longitude of EU's
300 emission is transported and deposited at 30-60°E in RU throughout the whole year and at 100-
301 120°E in EA in spring and fall. According to Fig. 4(c), SA exports its S emission to 30-60°E in
302 ME and eastern Africa in early spring and to 90°E-180° in EA and North Pacific Ocean from late
303 spring until fall. In particular, the influence on EA can reach $(5-10) \times 10^4 \text{ kg(S) month}^{-1}$ per 0.1°
304 longitude in mid-spring. According to Fig. 4(d), EA's S emission is widely transported and
305 deposited over the North Pacific Ocean throughout the whole year. The Asian outflow arrives at
306 the west coast of NA (~130°W) in all seasons except summer, but only reaches far in western



307 NA (~90°W) in spring and brings about 1×10^4 kg(S) month⁻¹ per 0.1° longitude of S deposition.
308 The monthly changes of NO_y deposition with perturbation experiments are shown in Fig. 5.
309 Compared to S deposition, the change in NO_y deposition by hemispheric transport is generally
310 smaller. For instance, the NA's impact on Eurasia is $(1-3) \times 10^4$ kg(S) month⁻¹ per 0.1° longitude
311 for S deposition, but is less than 0.5×10^4 kg(N) month⁻¹ per 0.1° longitude for NO_y deposition.
312 The SA's impact on EA (90-120°E) can reach $(5-10) \times 10^4$ kg(S) month⁻¹ per 0.1° longitude for S
313 deposition, but the amount is 4 times lower for NO_y deposition. This result is in accordance with
314 the S-R results in section 3.1 that more S emission is transported out of the source regions than N
315 emission, due to higher emission altitudes and longer chemical lifetimes. Patterns similar to NO_y
316 are also found in the monthly changes of NH_x deposition (Fig. S3).

317 The deposition change via transport between neighboring regions is found throughout the
318 whole year and is slightly stronger in winter, such as between EU and RU (~30°E) (Fig. 4(b) and
319 (f)) and from EA to the North Pacific Ocean (~130°E) (Fig. 4(d)). This is consistent with the
320 seasonality we found for the export of emission by source regions in section 3.1. In addition,
321 most source regions reduce more S and NO_x emissions in winter than the other seasons (Table
322 S3), thus more emissions are exported abroad in winter. On the contrary, most of the deposition
323 change by transport over long distance occurs in spring and fall, especially for the hemispheric
324 transport from NA to EU, from EU to EA and from EA to NA. This agrees with the seasonality
325 of the transpacific, transatlantic and trans-Eurasia flows of air pollutants (Holzer et al., 2005; Liu
326 et al., 2005; Liang et al., 2004; Brown-Steiner and Hess, 2011; Li et al., 2014; Auvray and Bey,
327 2005; Wild et al., 2004; Liu et al., 2003). The long distance transport of emissions is low in winter,
328 due to that the formation of secondary species like PAN is suppressed due to slow oxidation
329 (Berntsen et al., 1999; Deolal et al., 2013; Moxim et al., 1996), which plays an important role as a
330 reservoir for NO_x in the long-range transport of air pollution (Lin et al., 2010; Hudman et al.,
331 2004).

332 3.3 Own region and foreign contributions on deposition

333 This section compares the contributions of hemispheric transport and own region emission
334 control on deposition. The second metric is the response to extra-regional emission reduction
335 (RERER) as shown in Table 2. It is calculated by dividing the Δ Depo due to foreign emission



336 reduction by Δ Depo due to global (foreign + own region) emission control following equation
337 (2).

$$338 \quad RERER_i = \frac{\Delta Depo_i (foreign)}{\Delta Depo_i (global)} \quad (2)$$

339 where i is the region of focus. Δ Depo _{i} (foreign) is the Δ Depo in region i due to 20% foreign
340 emission reduction. It is calculated by subtracting the Δ Depo due to 20% own region emission
341 change from Δ Depo due to 20% global emission change. Δ Depo _{i} (global) is the Δ Depo in
342 region i due to 20% global emission reduction. This metric compares the contributions from
343 foreign emission reduction with own region emission control on local deposition. A low RERER
344 value (close to 0) indicates a predominance impact of own region emission on local deposition,
345 while high RERER value (close to 1) means strong impact of hemispheric transport on local
346 deposition.

347 The total column includes both non-coastal and coastal regions. As we expected, NA
348 (0.07-0.17), SA (0.04-0.18) and EA (0.16) regions have relatively low RERER values, due to
349 large emissions and deposition in those regions compared to the foreign contributions. EU (0.12-
350 0.36) and ME (0.32-0.42) have relatively higher RERER values. RU is the only region with
351 RERER (0.55-0.61) higher than 0.5, which means its deposition is almost equally sensitive to
352 foreign impact and own region control. The RERER values of S deposition and NO_y deposition
353 are of similar magnitudes, while the RERER of NH_x deposition is 0.1 lower, due to the lack of
354 contribution from EA.

355 For non-coastal regions, the own region impact includes control of both its coastal and
356 non-coastal regions. The foreign impact comes from emission reduction of foreign coastal and
357 non-coastal regions. The RERER values of coastal regions are generally 0.1-0.3 higher than
358 those of non-coastal regions. In particular, the values for RU's coast are all higher than 0.84.
359 Even regions with low total RERER such as NA and SA have high RERER on coastal regions.
360 For instance, the RERER of NA reached 0.3-0.4 for its coastal region, more than double of the
361 RERER on its non-coastal regions (0.05-0.12). Coastal regions receive high proportion of
362 deposition from foreign transport. According to table 1, EA exports 5% of its S and N emission
363 to RU, almost half of which is deposited on RU's coastal regions. RU exports 7-12% of S and N
364 emission to EA, of which 30% is deposited on EU's coastal regions. The impact of hemispheric



365 transport is identical or even larger than the effect of own region emission control for some
366 coastal or near coastal regions. According to Fig. 2, 20% emission reduction in EA can reduce 2-
367 5% of S deposition in the west coast of NA. This effect is even larger than 20% emission
368 reduction in NA (<1%). Similarly, 20% emission reduction in NA can change 2-5% of S
369 deposition in west coast of EU, which is almost identical to the effect of 20% emission control in
370 EU. On one hand, the emissions in western NA and western EU are relatively low, thus the effect
371 of own region control is not significant. On the other hand, these coastal regions are in the
372 downwind location of eastern EA and eastern NA, which are the main source regions of S and N
373 emissions. Coastal regions serve as transit places for air-sea exchange with vulnerable ecosystem
374 (Jickells, 2006;Jickells et al., 2017). The over-richness of deposition in coastal water and
375 ecosystem can evoke a number of environmental issues, of which some are specifically for
376 coastal regions such as threats to coastal benthic and planktonic system and sustainability of
377 fishery (Paerl, 2002;Doney et al., 2007).

378 Figure 6 compares the foreign and own region contributions on own region deposition.
379 Other (OTH, pattern fill in the figure) is calculated as $\Delta \text{Depo}_{(\text{GLO})} - \sum \Delta \text{Depo}_{(\text{case})}$ (case = 6,
380 including NA, EU, SA, EA, ME and RU). It indicates the deposition change in the receptor
381 region due to other reasons than the sum of separate emission reduction in the 6 regions. For
382 regions with low RERER values (NA, SA and EA), the own region emission dominates the
383 deposition by more than 80%. For these regions, determined by vicinity and transport patterns,
384 the foreign impact is somewhat dominated by certain source regions, such as from EA to NA (2-
385 4% out of 4-5%), from ME to SA (5-6% out of 7-11%) and from SA to EA (3-4% out of 4-7%).
386 For EU and ME, there is about 20% contribution from “OTH”. It could come from the emission
387 reduction in rest of world, especially nearby regions such as Central Asia and North Africa. It
388 could also come from the joint effects of emission control by multiple source regions. However,
389 the model simulations do not allow to separate these two contributions in this study. Beside this,
390 RU contributes 4-5% to EU’s deposition and EU contributes 5% to ME’s deposition. For high
391 RERER regions, RU has a different pattern than the other regions. The contributions of
392 hemispheric transport from other 5 regions (23-45%) are almost equivalent to its own region
393 emission control (39-45%). There are significant contributions from EA (20-24%) and EU (13-
394 15%), which is reasonable since RU emits low S and N emissions, but is located close to these
395 two major source regions.



396 Fig. 7 shows the inter-model variation on simulating the changes of deposition of SO_x ,
397 NO_y , and NH_x under emission perturbation cases, separate for wet and dry deposition. The
398 values are global integrated changes in component deposition for perturbation experiments from
399 MMM results with error bars showing the maximum and minimum values of models. The figure
400 only shows main compositions of S and N deposition, which together account for more than 95%
401 of total deposition. In terms of S deposition (Fig. 7(a)), the differences between the maximum
402 and minimum values of models for different perturbation cases range from $\pm(0.03\text{--}0.13)$ Tg(S)
403 ($\pm 29\text{--}83\%$ of MMM), $\pm(0.00\text{--}0.11)$ Tg(S) ($\pm 39\text{--}78\%$), $\pm(0.00\text{--}0.01)$ Tg(S) ($\pm 21\text{--}57\%$) and $\pm(0.01\text{--}$
404 $0.09)$ Tg(S) ($\pm 11\text{--}51\%$) for SO_2 dry and wet deposition and SO_4^{2-} dry and wet deposition,
405 respectively. High uncertainty is found in EA perturbation case, where the model divergence are
406 mainly found on SO_2 wet and dry deposition and SO_4^{2-} wet deposition. In terms of NO_y
407 deposition (Fig. 5(b)), the differences among cases are about $\pm(0.00\text{--}0.05)$ Tg(N) ($\pm 16\text{--}39\%$),
408 $\pm(0.02\text{--}0.28)$ Tg(N) ($\pm 23\text{--}70\%$) and $\pm(0.02\text{--}0.47)$ Tg(N) ($\pm 15\text{--}45\%$) for NO_2 dry deposition and
409 NO_3^- dry and wet deposition, respectively. The EA case also has the largest inter-model
410 variation, with high uncertainty in simulating both the NO_3^- wet and dry deposition. In terms of
411 NH_x deposition (Fig. 5(c)), the differences are about $\pm(0.00\text{--}0.06)$ Tg(N) ($\pm 2\text{--}27\%$), $\pm(0.00\text{--}0.08)$
412 Tg(N) ($\pm 10\text{--}55\%$) and $\pm(0.01\text{--}0.06)$ Tg(N) ($\pm 5\%$) for NH_3 dry deposition and NH_4^+ dry and wet
413 deposition, respectively. Both EA and SA have relatively high uncertainties on NH_4^+ dry
414 deposition. Overall, the inter-model variation is considerably high for the deposition change
415 under EA emission perturbation. On one hand, the EA perturbation case assumes the largest
416 amount of emission reductions among all cases (Table S3). On the other hand, model evaluation
417 (Tan et al., 2018) also has reported high model bias in simulating the deposition in this region,
418 and suggest an incomplete knowledge from the combined picture provided by observations and
419 models.

420 4 Conclusion

421 This study assesses the impact of hemispheric transport on S and N deposition for 6 regions:
422 North America, Europe, South Asia, East Asia, Russia and Middle East, by using multi-model
423 ensemble results from 11 models of HTAP II project, with simulations under base case and 20%
424 emission reduction scenarios.



425 We investigate the export of S and N emissions by source regions. Results show that
426 about 27-58%, 26-46% and 12-23% of the emitted S, NO_x and NH₃ emissions are deposited
427 outside of the source regions. The most significant exports of emissions are from Europe to
428 Russia (10-14%), from South Asia to East Asia (4-9%), from East Asia to Russia (5%) and from
429 Russia to Europe (7-12%) and East Asia (4-5%). Most regions export 5-10% more emission to
430 abroad in winter than summer, which is highly influenced by chemistry, precipitation amount
431 and frequency, atmospheric mixing and transport patterns.

432 We explore the impact of hemispheric transport on deposition in receptor regions.
433 Overall, 20% emission reduction in source regions could affect 1-10% of deposition on foreign
434 continental regions and 1-15% on foreign coastal regions and open ocean, especially from North
435 America to the North Atlantic Ocean (5-15%), from South Asia to western East Asia (2-10%)
436 and from East Asia to North Pacific Ocean (5-15%) and western North America (5-8%). The
437 amounts of deposition brought by hemispheric transport range from 10⁴-10⁵ kg(S or N) month⁻¹
438 per 0.1° longitude (meridional sum). The impact on deposition via transport between
439 neighbouring regions (i.e. Europe and Russia) is generally found throughout the whole year and
440 slightly stronger in winter, while that via transport over long distance (i.e. from East Asia to
441 North America) mainly takes place in spring and fall.

442 We compare the own region and foreign impact on deposition. The deposition in North
443 America, South Asia and East Asia is dominated (~80%) by their own region emission, while
444 Europe, Middle East and Russia receive 40-60% of impact from hemispheric transport. In
445 particular, Russian deposition is even equally sensitive to foreign inputs and own region
446 emission, with high contributions from two neighbouring source regions: East Asia (~20%) and
447 Europe (~15%). Coastal regions receive upmost half of the hemispheric transport from foreign
448 regions. Deposition in coastal regions or near-coastal open ocean is found twice more sensitive
449 to long-range transport than non-coastal regions. For some coastal regions such as west coast of
450 North America and west coast of Europe, the impact of hemispheric transport is identical or even
451 larger than that of own region emission control.

452 This study highlights the impact of hemispheric transport on deposition in coastal regions
453 and open ocean, which hasn't been fully studied in the literature. We therefore suggest further
454 research on this impact on the mitigation of coastal and oceanic ecosystem, with regards to the
455 increasing concentration of air pollutants in hemispheric outflow. We also find significant impact



456 of hemispheric transport on deposition in relatively low emission regions such as Russia. The
457 impact on their ecosystem and human health requires further research. Meanwhile, there is still a
458 portion of foreign impact that hasn't been attributed in this study (aggregated as other regions
459 "OTH" in Fig. 6). Some regions are not included in perturbation experiments, but are found with
460 large impact by/to other regions. For instance, at least 4 regions (North America, Europe, South
461 Asia and Middle East) have shown considerable impact (2-10%) on the S and N deposition in
462 North Africa. The impact from/by Southeast Asia is also unknown, which is regarded as a big
463 contributor of global S and N emissions in Asia. We suggest the future HTAP simulations to
464 include these regions in the perturbation experiments.

465

466 *Acknowledgements.* We thank all participating modelling groups in HTAP II for providing the
467 simulation data. The National Center for Atmospheric Research (NCAR) is funded by the
468 National Science Foundation. The CESM project is supported by the National Science
469 Foundation and the Office of Science (BER) of the U.S. Department of Energy. Computing
470 resources were provided by the Climate Simulation Laboratory at NCAR's Computational and
471 Information Systems Laboratory (CISL), sponsored by the National Science Foundation and
472 other agencies. Supercomputer system of the National Institute for Environmental Studies, Japan.
473 The Environment Research and Technology Development Fund (S-12-3) of the Ministry of the
474 Environment, Japan. JSPS KAKENHI grants 15H01728.

475

476

477 **References**

- 478 Arndt, R. L., and Carmichael, G. R.: Long-range transport and deposition of sulfur in Asia,
479 *Water Air and Soil Pollution*, 85, 2283-2288, 1995.
- 480 Auvray, M., and Bey, I.: Long-range transport to Europe: Seasonal variations and implications
481 for the European ozone budget, *J Geophys Res-Atmos*, 110, 2005.
- 482 Bergstrom, A. K., and Jansson, M.: Atmospheric nitrogen deposition has caused nitrogen
483 enrichment and eutrophication of lakes in the northern hemisphere, *Global Change Biol*, 12,
484 635-643, 10.1111/j.1365-2486.2006.01129.x, 2006.
- 485 Berntsen, T. K., Karlsdottir, S., and Jaffe, D. A.: Influence of Asian emissions on the
486 composition of air reaching the North Western United States, *Geophys Res Lett*, 26, 2171-
487 2174, 1999.
- 488 Bey, I., Jacob, D. J., Logan, J. A., and Yantosca, R. M.: Asian chemical outflow to the Pacific in
489 spring: Origins, pathways, and budgets, *J Geophys Res-Atmos*, 106, 23097-23113,
490 10.1029/2001jd000806, 2001.
- 491 Bleeker, A., Hicks, W. K., Dentener, E., Galloway, J., and Erisman, J. W.: N deposition as a
492 threat to the World's protected areas under the Convention on Biological Diversity, *Environ*
493 *Pollut*, 159, 2280-2288, 2011.
- 494 Bobbink, R., Hicks, K., Galloway, J., Spranger, T., Alkemade, R., Ashmore, M., Bustamante, M.,
495 Cinderby, S., Davidson, E., Dentener, F., Emmett, B., Erisman, J. W., Fenn, M., Gilliam, F.,
496 Nordin, A., Pardo, L., and De Vries, W.: Global assessment of nitrogen deposition effects on
497 terrestrial plant diversity: a synthesis, *Ecol. Appl.*, 20, 30-59, 10.1890/08-1140.1, 2010.
- 498 Bouwman, A. F., Van Vuuren, D. P., Derwent, R. G., and Posch, M.: A global analysis of
499 acidification and eutrophication of terrestrial ecosystems, *Water Air and Soil Pollution*, 141,
500 349-382, 10.1023/a:1021398008726, 2002.
- 501 Brown-Steiner, B., and Hess, P.: Asian influence on surface ozone in the United States: A
502 comparison of chemistry, seasonality, and transport mechanisms, *J Geophys Res-Atmos*, 116,
503 10.1029/2011jd015846, 2011.
- 504 Clark, C. M., and Tilman, D.: Loss of plant species after chronic low-level nitrogen deposition to
505 prairie grasslands, *Nature*, 451, 712-715, 2008.
- 506 Dentener, F., Drevet, J., Lamarque, J. F., Bey, I., Eickhout, B., Fiore, A. M., Hauglustaine, D.,
507 Horowitz, L. W., Krol, M., Kulshrestha, U. C., Lawrence, M., Galy-Lacaux, C., Rast, S.,
508 Shindell, D., Stevenson, D., Van Noije, T., Atherton, C., Bell, N., Bergman, D., Butler, T.,
509 Cofala, J., Collins, B., Doherty, R., Ellingsen, K., Galloway, J., Gauss, M., Montanaro, V.,
510 Muller, J. F., Pitari, G., Rodriguez, J., Sanderson, M., Solmon, F., Strahan, S., Schultz, M.,
511 Sudo, K., Szopa, S., and Wild, O.: Nitrogen and sulfur deposition on regional and global
512 scales: A multimodel evaluation, *Global Biogeochem Cy*, 20, 21, 10.1029/2005gb002672,
513 2006.
- 514 Deolal, S. P., Staehelin, J., Brunner, D., Cui, J. B., Steinbacher, M., Zellweger, C., Henne, S.,
515 and Vollmer, M. K.: Transport of PAN and NO_y from different source regions to the Swiss
516 high alpine site Jungfraujoch, *Atmospheric Environment*, 64, 103-115,
517 10.1016/j.atmosenv.2012.08.021, 2013.
- 518 Derwent, R. G., Stevenson, D. S., Collins, W. J., and Johnson, C. E.: Intercontinental transport
519 and the origins of the ozone observed at surface sites in Europe, *Atmospheric Environment*,
520 38, 1891-1901, 10.1016/j.atmosenv.2004.01.008, 2004.
- 521 Doney, S. C., Mahowald, N., Lima, I., Feely, R. A., Mackenzie, F. T., Lamarque, J. F., and
522 Rasch, P. J.: Impact of anthropogenic atmospheric nitrogen and sulfur deposition on ocean



- 523 acidification and the inorganic carbon system, Proceedings of the National Academy of
524 Sciences of the United States of America, 104, 14580-14585, 10.1073/pnas.0702218104,
525 2007.
- 526 Duce, R. A., LaRoche, J., Altieri, K., Arrigo, K. R., Baker, A. R., Capone, D. G., Cornell, S.,
527 Dentener, F., Galloway, J., Ganeshram, R. S., Geider, R. J., Jickells, T., Kuypers, M. M.,
528 Langlois, R., Liss, P. S., Liu, S. M., Middelburg, J. J., Moore, C. M., Nickovic, S., Oschlies,
529 A., Pedersen, T., Prospero, J., Schlitzer, R., Seitzinger, S., Sorensen, L. L., Uematsu, M.,
530 Ulloa, O., Voss, M., Ward, B., and Zamora, L.: Impacts of atmospheric anthropogenic
531 nitrogen on the open ocean, *Science*, 320, 893-897, 10.1126/science.1150369, 2008.
- 532 Duncan, B. N., and Bey, I.: A modeling study of the export pathways of pollution from Europe:
533 Seasonal and interannual variations (1987-1997), *J Geophys Res-Atmos*, 109, 2004.
- 534 Duncan, B. N., West, J. J., Yoshida, Y., Fiore, A. M., and Ziemke, J. R.: The influence of
535 European pollution on ozone in the Near East and northern Africa, *Atmospheric Chemistry
536 and Physics*, 8, 2267-2283, 2008.
- 537 Fiore, A. M., Dentener, F. J., Wild, O., Cuvelier, C., Schultz, M. G., Hess, P., Textor, C., Schulz,
538 M., Doherty, R. M., Horowitz, L. W., MacKenzie, I. A., Sanderson, M. G., Shindell, D. T.,
539 Stevenson, D. S., Szopa, S., Van Dingenen, R., Zeng, G., Atherton, C., Bergmann, D., Bey, I.,
540 Carmichael, G., Collins, W. J., Duncan, B. N., Faluvegi, G., Folberth, G., Gauss, M., Gong,
541 S., Hauglustaine, D., Holloway, T., Isaksen, I. S. A., Jacob, D. J., Jonson, J. E., Kaminski, J.
542 W., Keating, T. J., Lupu, A., Marmer, E., Montanaro, V., Park, R. J., Pitari, G., Pringle, K. J.,
543 Pyle, J. A., Schroeder, S., Vivanco, M. G., Wind, P., Wojcik, G., Wu, S., and Zuber, A.:
544 Multimodel estimates of intercontinental source-receptor relationships for ozone pollution,
545 *Journal of Geophysical Research*, 114, 10.1029/2008jd010816, 2009.
- 546 Fu, J. S., Dong, X. Y., Gao, Y., Wong, D. C., and Lam, Y. F.: Sensitivity and linearity analysis
547 of ozone in East Asia: The effects of domestic emission and intercontinental transport,
548 *Journal of the Air & Waste Management Association*, 62, 13,
549 10.1080/10962247.2012.699014, 2012.
- 550 Galloway, J. N., Townsend, A. R., Erisman, J. W., Bekunda, M., Cai, Z. C., Freney, J. R.,
551 Martinelli, L. A., Seitzinger, S. P., and Sutton, M. A.: Transformation of the nitrogen cycle:
552 Recent trends, questions, and potential solutions, *Science*, 320, 889-892,
553 10.1126/science.1136674, 2008.
- 554 Galmarini, S., Koffi, B., Solazzo, E., Keating, T., Hogrefe, C., Schulz, M., Benedictow, A.,
555 Griesfeller, J. J., Janssens-Maenhout, G., Carmichael, G., Fu, J., and Dentener, F.: Technical
556 note: Coordination and harmonization of the multi-scale, multi-model activities HTAP2,
557 AQMEII3, and MICS-Asia3: simulations, emission inventories, boundary conditions, and
558 model output formats, *Atmos. Chem. Phys.*, 17, 1543-1555, 10.5194/acp-17-1543-2017,
559 2017.
- 560 Glotfelty, T., Zhang, Y., Karamchandani, P., and Streets, D. G.: Will the role of intercontinental
561 transport change in a changing climate?, *Atmospheric Chemistry and Physics*, 14, 9379-9402,
562 10.5194/acp-14-9379-2014, 2014.
- 563 Guerova, G., Bey, I., Attie, J. L., Martin, R. V., Cui, J., and Sprenger, M.: Impact of transatlantic
564 transport episodes on summertime ozone in Europe, *Atmospheric Chemistry and Physics*, 6,
565 2057-2072, 2006.
- 566 Guo, J. H., Liu, X. J., Zhang, Y., Shen, J. L., Han, W. X., Zhang, W. F., Christie, P., Goulding, K.
567 W. T., Vitousek, P. M., and Zhang, F. S.: Significant Acidification in Major Chinese
568 Croplands, *Science*, 327, 1008-1010, 2010.



- 569 Holzer, M., Hall, T. M., and Stull, R. B.: Seasonality and weather-driven variability of
570 transpacific transport, *J Geophys Res-Atmos*, 110, 10.1029/2005jd006261, 2005.
- 571 Hudman, R. C., Jacob, D. J., Cooper, O. R., Evans, M. J., Heald, C. L., Park, R. J., Fehsenfeld, F.,
572 Flocke, F., Holloway, J., Hubler, G., Kita, K., Koike, M., Kondo, Y., Neuman, A., Nowak, J.,
573 Oltmans, S., Parrish, D., Roberts, J. M., and Ryerson, T.: Ozone production in transpacific
574 Asian pollution plumes and implications for ozone air quality in California, *J Geophys Res-*
575 *Atmos*, 109, 2004.
- 576 Jacob, D. J., Logan, J. A., and Murti, P. P.: Effect of rising Asian emissions on surface ozone in
577 the United States, *Geophys Res Lett*, 26, 2175-2178, 10.1029/1999gl000450, 1999.
- 578 Jaffe, D., Price, H., Parrish, D., Goldstein, A., and Harris, J.: Increasing background ozone
579 during spring on the west coast of North America, *Geophys Res Lett*, 30,
580 10.1029/2003gl017024, 2003.
- 581 Janssens, I. A., Dieleman, W., Luyssaert, S., Subke, J. A., Reichstein, M., Ceulemans, R., Ciais,
582 P., Dolman, A. J., Grace, J., Matteucci, G., Papale, D., Piao, S. L., Schulze, E. D., Tang, J.,
583 and Law, B. E.: Reduction of forest soil respiration in response to nitrogen deposition, *Nature*
584 *Geoscience*, 3, 315-322, 10.1038/ngeo844, 2010.
- 585 Janssens-Maenhout, G., Crippa, M., Guizzardi, D., Dentener, F., Muntean, M., Pouliot, G.,
586 Keating, T., Zhang, Q., Kurokawa, J., Wankmuller, R., van der Gon, H. D., Kuenen, J. J. P.,
587 Klimont, Z., Frost, G., Darras, S., Koffi, B., and Li, M.: HTAP_v2.2: a mosaic of regional
588 and global emission grid maps for 2008 and 2010 to study hemispheric transport of air
589 pollution, *Atmospheric Chemistry and Physics*, 15, 11411-11432, 10.5194/acp-15-11411-
590 2015, 2015.
- 591 Jickells, T.: The role of air-sea exchange in the marine nitrogen cycle, *Biogeosciences*, 3, 271-
592 280, 2006.
- 593 Jickells, T. D., Buitenhuis, E., Altieri, K., Baker, A. R., Capone, D., Duce, R. A., Dentener, F.,
594 Fennel, K., Kanakidou, M., LaRoche, J., Lee, K., Liss, P., Middelburg, J. J., Moore, J. K.,
595 Okin, G., Oschlies, A., Sarin, M., Seitzinger, S., Sharples, J., Singh, A., Suntharalingam, P.,
596 Uematsu, M., and Zamora, L. M.: A reevaluation of the magnitude and impacts of
597 anthropogenic atmospheric nitrogen inputs on the ocean, *Global Biogeochem Cy*, 31, 289-
598 305, 2017.
- 599 Kanakidou, M., Myriokefalitakis, S., Daskalakis, N., Fanourgakis, G., Nenes, A., Baker, A. R.,
600 Tsigaridis, K., and Mihalopoulos, N.: Past, Present, and Future Atmospheric Nitrogen
601 Deposition, *Journal of the Atmospheric Sciences*, 73, 2039-2047, 10.1175/jas-d-15-0278.1,
602 2016.
- 603 Kim, T. W., Lee, K., Najjar, R. G., Jeong, H. D., and Jeong, H. J.: Increasing N Abundance in
604 the Northwestern Pacific Ocean Due to Atmospheric Nitrogen Deposition, *Science*, 334, 505-
605 509, 2011.
- 606 Lamarque, J. F., Kiehl, J. T., Brasseur, G. P., Butler, T., Cameron-Smith, P., Collins, W. D.,
607 Collins, W. J., Granier, C., Hauglustaine, D., Hess, P. G., Holland, E. A., Horowitz, L.,
608 Lawrence, M. G., McKenna, D., Merilees, P., Prather, M. J., Rasch, P. J., Rotman, D.,
609 Shindell, D., and Thornton, P.: Assessing future nitrogen deposition and carbon cycle
610 feedback using a multimodel approach: Analysis of nitrogen deposition, *J Geophys Res-*
611 *Atmos*, 110, 10.1029/2005jd005825, 2005.
- 612 Lamarque, J. F., Dentener, F., McConnell, J., Ro, C. U., Shaw, M., Vet, R., Bergmann, D.,
613 Cameron-Smith, P., Dalsoren, S., Doherty, R., Faluvegi, G., Ghan, S. J., Josse, B., Lee, Y. H.,
614 MacKenzie, I. A., Plummer, D., Shindell, D. T., Skeie, R. B., Stevenson, D. S., Strode, S.,



- 615 Zeng, G., Curran, M., Dahl-Jensen, D., Das, S., Fritzsche, D., and Nolan, M.: Multi-model
616 mean nitrogen and sulfur deposition from the Atmospheric Chemistry and Climate Model
617 Intercomparison Project (ACCMIP): evaluation of historical and projected future changes,
618 Atmospheric Chemistry and Physics, 13, 7997-8018, 10.5194/acp-13-7997-2013, 2013.
- 619 Li, Q. B., Jacob, D. J., Bey, I., Palmer, P. I., Duncan, B. N., Field, B. D., Martin, R. V., Fiore, A.
620 M., Yantosca, R. M., Parrish, D. D., Simmonds, P. G., and Oltmans, S. J.: Transatlantic
621 transport of pollution and its effects on surface ozone in Europe and North America, J
622 Geophys Res-Atmos, 107, 10.1029/2001jd001422, 2002.
- 623 Li, Q. B., Jacob, D. J., Munger, J. W., Yantosca, R. M., and Parrish, D. D.: Export of NO_y from
624 the North American boundary layer: Reconciling aircraft observations and global model
625 budgets, J Geophys Res-Atmos, 109, 2004.
- 626 Li, X. Y., Liu, J. F., Mauzerall, D. L., Emmons, L. K., Walters, S., Horowitz, L. W., and Tao, S.:
627 Effects of trans-Eurasian transport of air pollutants on surface ozone concentrations over
628 Western China, J Geophys Res-Atmos, 119, 12338-12354, 10.1002/2014jd021936, 2014.
- 629 Liang, Q., Jaegle, L., Jaffe, D. A., Weiss-Penzias, P., Heckman, A., and Snow, J. A.: Long-range
630 transport of Asian pollution to the northeast Pacific: Seasonal variations and transport
631 pathways of carbon monoxide, J Geophys Res-Atmos, 109, 2004.
- 632 Lin, M., Holloway, T., Carmichael, G. R., and Fiore, A. M.: Quantifying pollution inflow and
633 outflow over East Asia in spring with regional and global models, Atmospheric Chemistry
634 and Physics, 10, 4221-4239, 10.5194/acp-10-4221-2010, 2010.
- 635 Liu, H. Y., Jacob, D. J., Bey, I., Yantosca, R. M., Duncan, B. N., and Sachse, G. W.: Transport
636 pathways for Asian pollution outflow over the Pacific: Interannual and seasonal variations, J
637 Geophys Res-Atmos, 108, 10.1029/2002jd003102, 2003.
- 638 Liu, J. F., Mauzerall, D. L., and Horowitz, L. W.: Analysis of seasonal and interannual
639 variability in transpacific transport, J Geophys Res-Atmos, 110, 10.1029/2004jd005207,
640 2005.
- 641 Lu, Z., Streets, D. G., Zhang, Q., Wang, S., Carmichael, G. R., Cheng, Y. F., Wei, C., Chin, M.,
642 Diehl, T., and Tan, Q.: Sulfur dioxide emissions in China and sulfur trends in East Asia since
643 2000, Atmospheric Chemistry and Physics, 10, 6311-6331, 2010.
- 644 Moxim, W. J., Levy, H., and Kasibhatla, P. S.: Simulated global tropospheric PAN: Its transport
645 and impact on NO_x, J Geophys Res-Atmos, 101, 12621-12638, 10.1029/96jd00338, 1996.
- 646 Paerl, H. W.: Connecting atmospheric nitrogen deposition to coastal eutrophication,
647 Environmental science & technology, 36, 323a-326a, 2002.
- 648 Parrish, D. D., Dunlea, E. J., Atlas, E. L., Schauffler, S., Donnelly, S., Stroud, V., Goldstein, A.
649 H., Millet, D. B., McKay, M., Jaffé, D. A., Price, H. U., Hess, P. G., Flocke, F., and Roberts,
650 J. M.: Changes in the photochemical environment of the temperate North Pacific troposphere
651 in response to increased Asian emissions, Journal of Geophysical Research: Atmospheres,
652 109, 10.1029/2004jd004978, 2004.
- 653 Parrish, D. D., Millet, D. B., and Goldstein, A. H.: Increasing ozone in marine boundary layer
654 inflow at the west coasts of North America and Europe, Atmospheric Chemistry and Physics,
655 9, 1303-1323, 2009.
- 656 Paulot, F., Jacob, D. J., and Henze, D. K.: Sources and Processes Contributing to Nitrogen
657 Deposition: An Adjoint Model Analysis Applied to Biodiversity Hotspots Worldwide,
658 Environmental science & technology, 47, 3226-3233, 10.1021/es3027727, 2013.
- 659 Phoenix, G. K., Hicks, W. K., Cinderby, S., Kuylenstierna, J. C. I., Stock, W. D., Dentener, F. J.,
660 Giller, K. E., Austin, A. T., Lefroy, R. D. B., Gimeno, B. S., Ashmore, M. R., and Ineson, P.:



- 661 Atmospheric nitrogen deposition in world biodiversity hotspots: the need for a greater global
662 perspective in assessing N deposition impacts, *Global Change Biol*, 12, 470-476,
663 10.1111/j.1365-2486.2006.01104.x, 2006.
- 664 Reidmiller, D. R., Fiore, A. M., Jaffe, D. A., Bergmann, D., Cuvelier, C., Dentener, F. J., Duncan,
665 B. N., Folberth, G., Gauss, M., Gong, S., Hess, P., Jonson, J. E., Keating, T., Lupu, A.,
666 Marmer, E., Park, R., Schultz, M. G., Shindell, D. T., Szopa, S., Vivanco, M. G., Wild, O.,
667 and Zuber, A.: The influence of foreign vs. North American emissions on surface ozone in
668 the US, *Atmospheric Chemistry and Physics*, 9, 5027-5042, 2009.
- 669 Richter, A., Burrows, J. P., Nuss, H., Granier, C., and Niemeier, U.: Increase in tropospheric
670 nitrogen dioxide over China observed from space, *Nature*, 437, 129-132,
671 10.1038/nature04092, 2005.
- 672 Sanderson, M. G., Dentener, F. J., Fiore, A. M., Cuvelier, C., Keating, T. J., Zuber, A., Atherton,
673 C. S., Bergmann, D. J., Diehl, T., Doherty, R. M., Duncan, B. N., Hess, P., Horowitz, L. W.,
674 Jacob, D. J., Jonson, J. E., Kaminski, J. W., Lupu, A., MacKenzie, I. A., Mancini, E.,
675 Marmer, E., Park, R., Pitari, G., Prather, M. J., Pringle, K. J., Schroeder, S., Schultz, M. G.,
676 Shindell, D. T., Szopa, S., Wild, O., and Wind, P.: A multi-model study of the hemispheric
677 transport and deposition of oxidised nitrogen, *Geophys Res Lett*, 35, 10.1029/2008gl035389,
678 2008.
- 679 Stohl, A., Trainer, M., Ryerson, T. B., Holloway, J. S., and Parrish, D. D.: Export of NO_y from
680 the North American boundary layer during 1996 and 1997 North Atlantic Regional
681 Experiments, *J Geophys Res-Atmos*, 107, 2002.
- 682 Sudo, K., and Akimoto, H.: Global source attribution of tropospheric ozone: Long-range
683 transport from various source regions, *J Geophys Res-Atmos*, 112, 2007.
- 684 Tan, J., Fu, J. S., Dentener, F., Sun, J., Emmons, L., Tilmes, S., Sudo, K., Flemming, J., Jonson,
685 J. E., Gravel, S., Bian, H., Henze, D., Lund, M. T., Kucsera, T., Takemura, T., and Keating,
686 T.: Multi-model study of HTAP II on sulfur and nitrogen deposition, *Atmospheric Chemistry
687 and Physics Discussions*, 1-36, 10.5194/acp-2017-1121, 2018.
- 688 Tao, Z. N., Yu, H. B., and Chin, M.: Impact of transpacific aerosol on air quality over the United
689 States: A perspective from aerosol-cloud-radiation interactions, *Atmospheric Environment*,
690 125, 48-60, 10.1016/j.atmosenv.2015.10.083, 2016.
- 691 van der A, R. J., Peters, D. H. M. U., Eskes, H., Boersma, K. F., Van Roozendael, M., De Smedt,
692 I., and Kelder, H. M.: Detection of the trend and seasonal variation in tropospheric NO₂ over
693 China, *Journal of Geophysical Research*, 111, 10.1029/2005jd006594, 2006.
- 694 van der A, R. J., Eskes, H. J., Boersma, K. F., van Noije, T. P. C., Van Roozendael, M., De
695 Smedt, I., Peters, D. H. M. U., and Meijer, E. W.: Trends, seasonal variability and dominant
696 NO_x source derived from a ten year record of NO₂ measured from space, *Journal of
697 Geophysical Research*, 113, 10.1029/2007jd009021, 2008.
- 698 Verstraeten, W. W., Neu, J. L., Williams, J. E., Bowman, K. W., Worden, J. R., and Boersma, K.
699 F.: Rapid increases in tropospheric ozone production and export from China, *Nature
700 Geoscience*, 8, 690+, 10.1038/ngeo2493, 2015.
- 701 Vet, R., Artz, R. S., Carou, S., Shaw, M., Ro, C. U., Aas, W., Baker, A., Bowersox, V. C.,
702 Dentener, F., Galy-Lacaux, C., Hou, A., Pienaar, J. J., Gillett, R., Forti, M. C., Gromov, S.,
703 Hara, H., Khodzher, T., Mahowald, N. M., Nickovic, S., Rao, P. S. P., and Reid, N. W.: A
704 global assessment of precipitation chemistry and deposition of sulfur, nitrogen, sea salt, base
705 cations, organic acids, acidity and pH, and phosphorus, *Atmospheric Environment*, 93, 3-100,
706 10.1016/j.atmosenv.2013.10.060, 2014.



- 707 Wild, O., and Akimoto, H.: Intercontinental transport of ozone and its precursors in a three-
708 dimensional global CTM, *J Geophys Res-Atmos*, 106, 27729-27744, 10.1029/2000jd000123,
709 2001.
- 710 Wild, O., Pochanart, P., and Akimoto, H.: Trans-Eurasian transport of ozone and its precursors, *J*
711 *Geophys Res-Atmos*, 109, 10.1029/2003jd004501, 2004.
- 712 WMO, 2017: Global Atmosphere Watch Workshop on Measurement-Model Fusion for Global
713 Total Atmospheric Deposition (MMF-GTAD), GAW Report No. 234. Available at
714 https://www.wmo.int/pages/prog/arep/gaw/documents/FINAL_GAW_234_23_May.pdf
- 715 Yienger, J. J., Galanter, M., Holloway, T. A., Phadnis, M. J., Guttikunda, S. K., Carmichael, G.
716 R., Moxim, W. J., and Levy, H.: The episodic nature of air pollution transport from Asia to
717 North America, *J Geophys Res-Atmos*, 105, 26931-26945, 10.1029/2000jd900309, 2000.
- 718 Yu, H. B., Chin, M., West, J. J., Atherton, C. S., Bellouin, N., Bergmann, D., Bey, I., Bian, H. S.,
719 Diehl, T., Forberth, G., Hess, P., Schulz, M., Shindell, D., Takemura, T., and Tan, Q.: A
720 multimodel assessment of the influence of regional anthropogenic emission reductions on
721 aerosol direct radiative forcing and the role of intercontinental transport, *J Geophys Res-*
722 *Atmos*, 118, 700-720, 10.1029/2012jd018148, 2013.
- 723 Zhang, L., Jacob, D. J., Boersma, K. F., Jaffe, D. A., Olson, J. R., Bowman, K. W., Worden, J.
724 R., Thompson, A. M., Avery, M. A., Cohen, R. C., Dibb, J. E., Flock, F. M., Fuelberg, H. E.,
725 Huey, L. G., McMillan, W. W., Singh, H. B., and Weinheimer, A. J.: Transpacific transport
726 of ozone pollution and the effect of recent Asian emission increases on air quality in North
727 America: an integrated analysis using satellite, aircraft, ozonesonde, and surface observations,
728 *Atmospheric Chemistry and Physics*, 8, 6117-6136, 2008.
- 729 Zhang, L., Jacob, D. J., Kopacz, M., Henze, D. K., Singh, K., and Jaffe, D. A.: Intercontinental
730 source attribution of ozone pollution at western US sites using an adjoint method, *Geophys*
731 *Res Lett*, 36, 5, 10.1029/2009gl037950, 2009.
- 732 Zhang, L., Jacob, D. J., Knipping, E. M., Kumar, N., Munger, J. W., Carouge, C. C., van
733 Donkelaar, A., Wang, Y. X., and Chen, D.: Nitrogen deposition to the United States:
734 distribution, sources, and processes, *Atmospheric Chemistry and Physics*, 12, 4539-4554,
735 2012.
- 736 Zhang, Q., Streets, D. G., He, K., Wang, Y., Richter, A., Burrows, J. P., Uno, I., Jang, C. J.,
737 Chen, D., Yao, Z., and Lei, Y.: NO_x emission trends for China, 1995-2004: The view from
738 the ground and the view from space, *J Geophys Res-Atmos*, 112, 10.1029/2007jd008684,
739 2007.

740

741



742 Caption:

743 Fig. 1. Administration boundaries of regions and coastal areas. 6 Regions with perturbation
744 experiments: 3-North America (NA), 4-Europe (EU), 5-South Asia (SA), 6-East Asia (EA), 11-
745 Middle East (MD) and 14-Russia, Belarussia, Ukraine (RU). Other regions: 1-Global, 2-Ocean
746 (including Arctic), 7-Southeast Asia, 8-Australia, 9-North Africa, 10- Sub Saharan Africa, 12-
747 Mexico, Central America, Caribbean, Guyanas, Venezuela, Columbia (Central America), 13-
748 South America, 15-Central Asia and 17-Antarctic.

749 Fig. 2 The response of S deposition to 20% emission reduction in source regions. The values are
750 the percentage changes (%) in deposition calculated as (changes in deposition with 20%
751 emission reduction) / (base case deposition) × 100%. The unit is %.

752 Fig.3 Same as Fig.2 but for NO_y deposition. The unit is %.

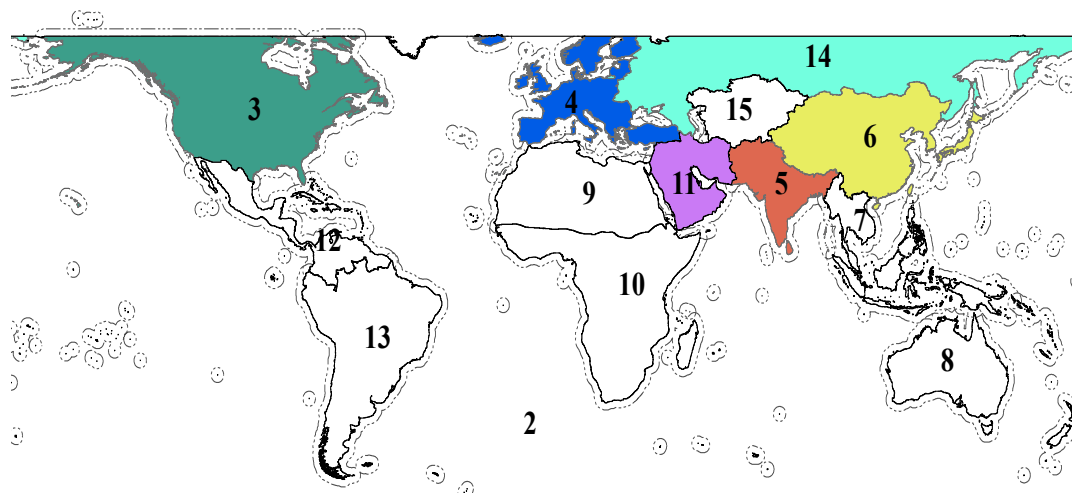
753 Fig. 4 The monthly changes of S deposition with 20% emission reduction in source regions. The
754 values are meridional total values versus time with a west-east resolution of 0.1 degree. The unit
755 is × 10⁴ kg(S) month⁻¹ per 0.1° longitude. The negative values indicate decline in deposition with
756 reduction in emission.

757 Fig. 5 Same as Fig.4 but for NO_y deposition. The unit is × 10⁴ kg(N) month⁻¹ per 0.1° longitude.

758 Fig. 6 Own region and foreign contributions on own region deposition. The values are calculated
759 by changes with 20% emission reduction. Other (OTH, pattern fill) is the contribution by other
760 reasons than emission reduction in the 6 regions (see text for details).

761 Fig. 7 Inter-model variations in deposition changes (unit: Tg(S or N) yr⁻¹) under emission
762 perturbation experiments. The values are MMM with error bars showing the max and min values
763 among all models.

764

765 **Fig. 1**

17

766

767 Fig. 1. Boundaries of regions and coastal areas (dashed). 6 Regions with perturbation

768 experiments: 3-North America (NA), 4-Europe (EU), 5-South Asia (SA), 6-East Asia (EA), 11-

769 Middle East (MD) and 14-Russia, Belarussia, Ukraine (RU). Other regions: 1-Global, 2-Ocean

770 (including Arctic), 7-Southeast Asia, 8-Australia, 9-North Africa, 10- Sub Saharan Africa, 12-

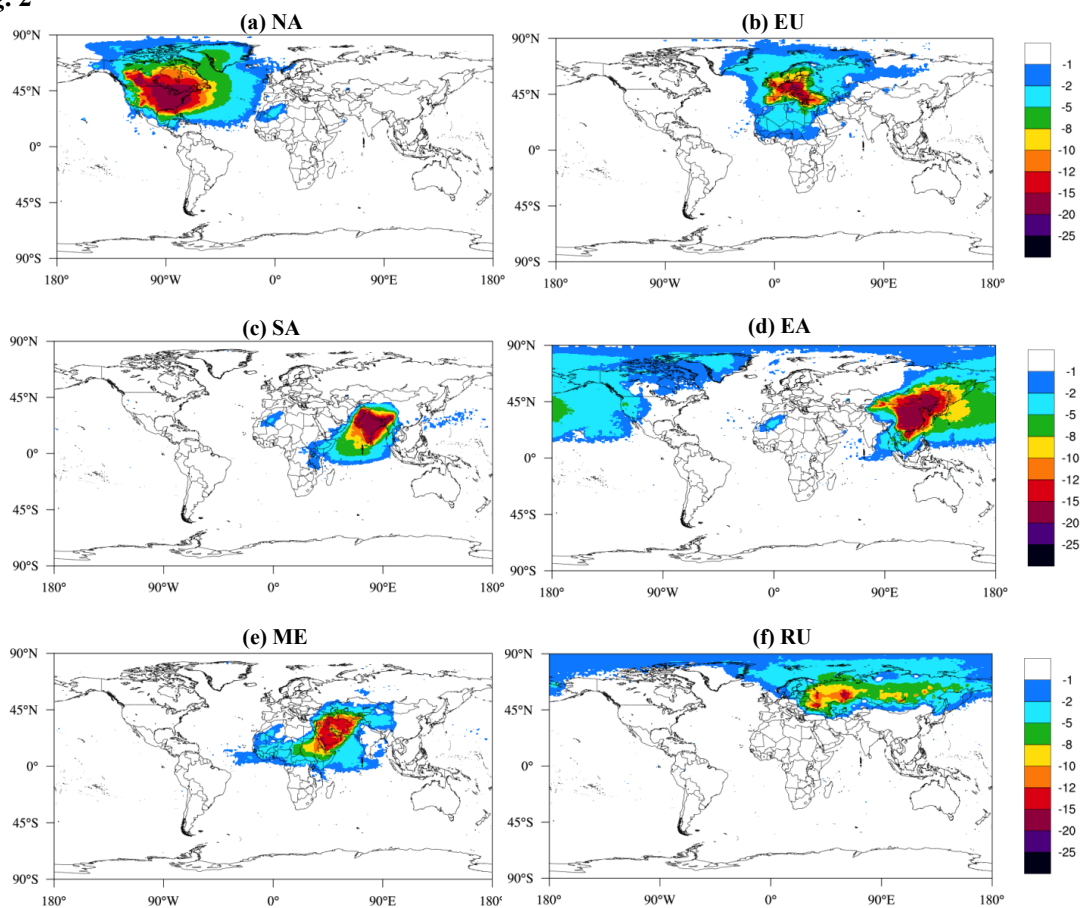
771 Mexico, Central America, Caribbean, Guyanas, Venezuela, Columbia (Central America), 13-

772 South America, 15-Central Asia and 17-Antarctic.

773



774 **Fig. 2**



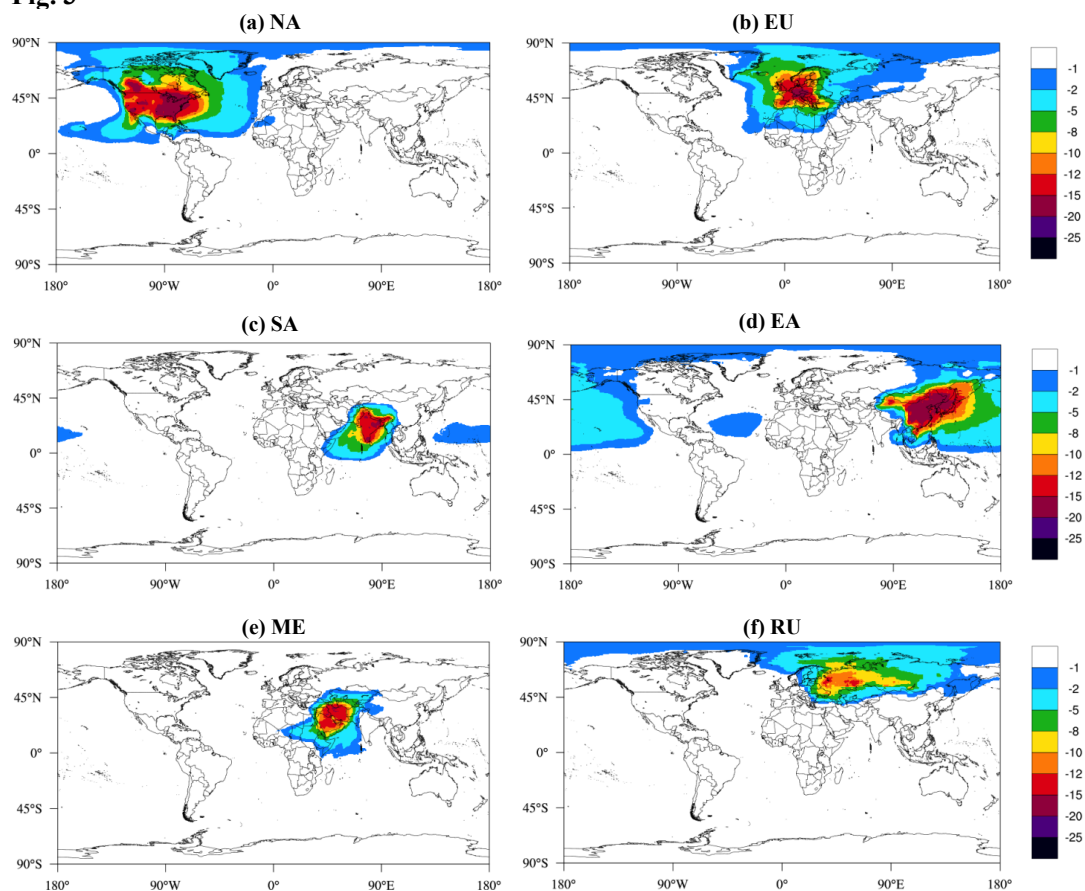
775

776 Fig. 2 The response of S deposition to 20% emission reduction in source regions. The values are
777 the percentage changes (%) in deposition calculated as (changes in deposition with 20%
778 emission reduction) / (base case deposition) × 100%. The unit is %.

779



780 **Fig. 3**

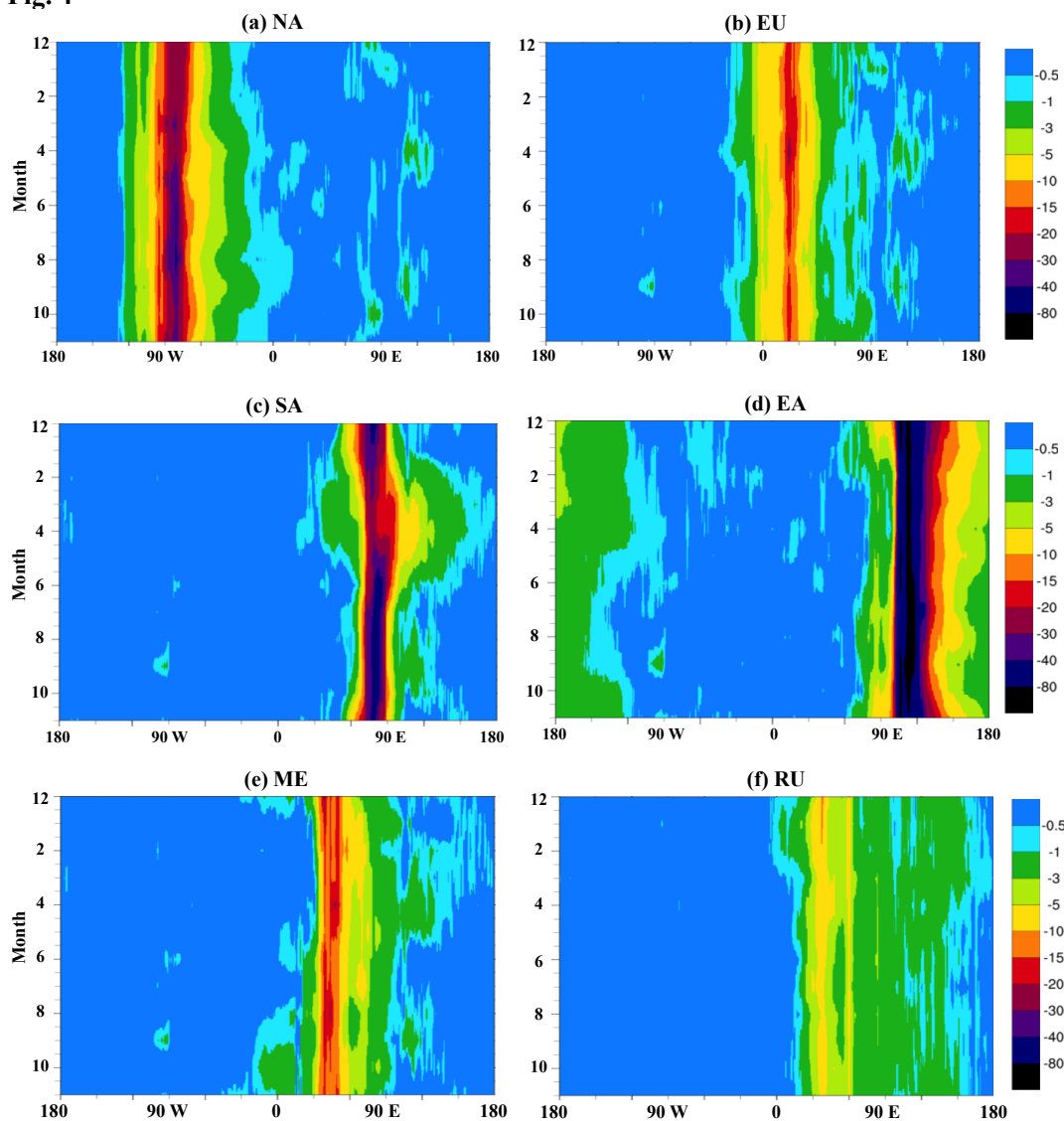


781
782
783

Fig.3 Same as Fig.2 but for NO_y deposition. The unit is %.



784 **Fig. 4**



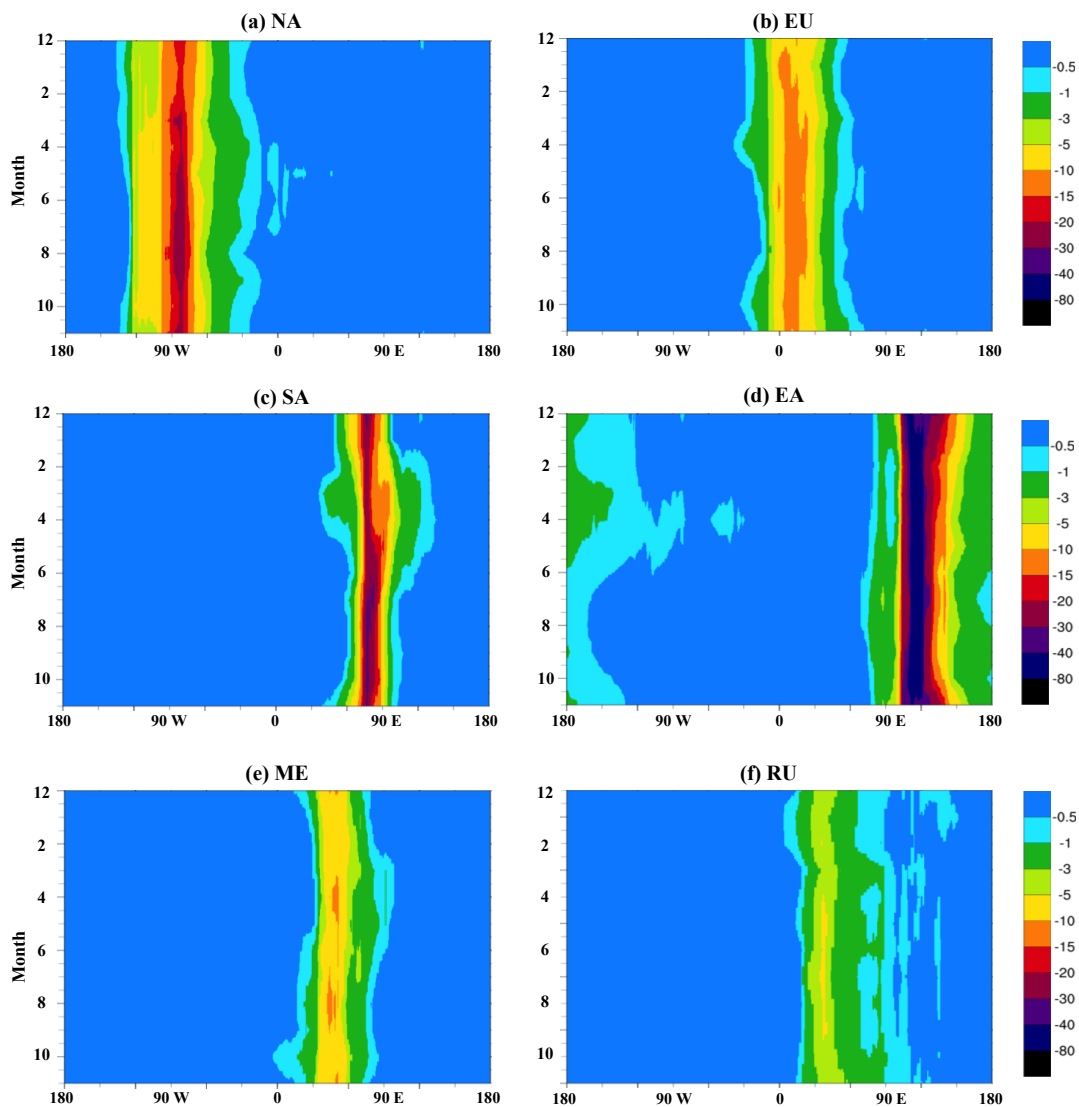
785

787 Fig. 4 The monthly changes of S deposition with 20% emission reduction in source regions. The
788 x-axis values are meridional total values versus time (y-axis) with a west-east resolution of 0.1
789 degree. The unit is $\times 10^4 \text{ kg(S) month}^{-1}$ per 0.1° longitude. Negative values indicate decline in
790 deposition with reduction in emission.

791



792 **Fig. 5**

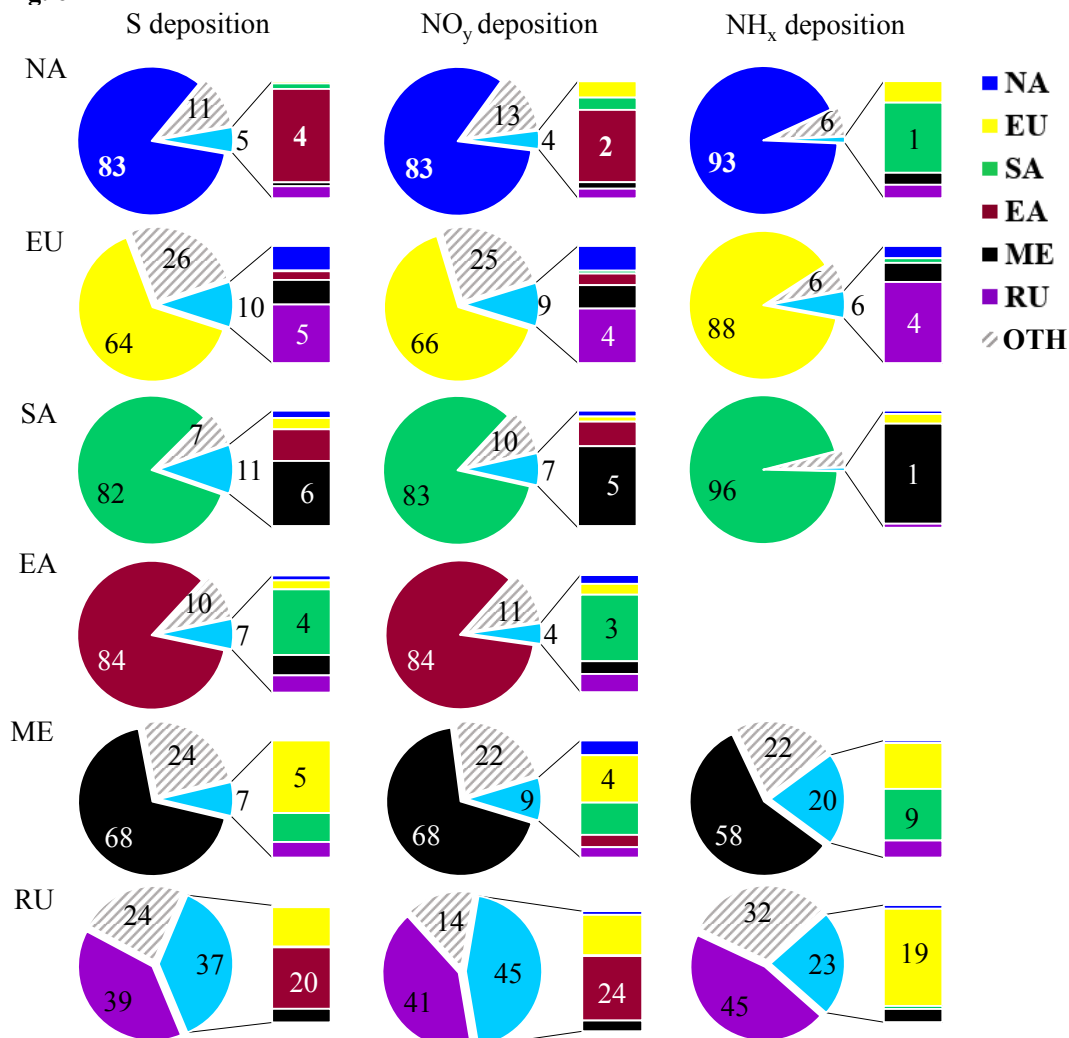


793
794
795

Fig. 5 Same as Fig.4 but for NO_y deposition. The unit is $\times 10^4 \text{ kg(N) month}^{-1}$ per 0.1° longitude.



796 **Fig. 6**

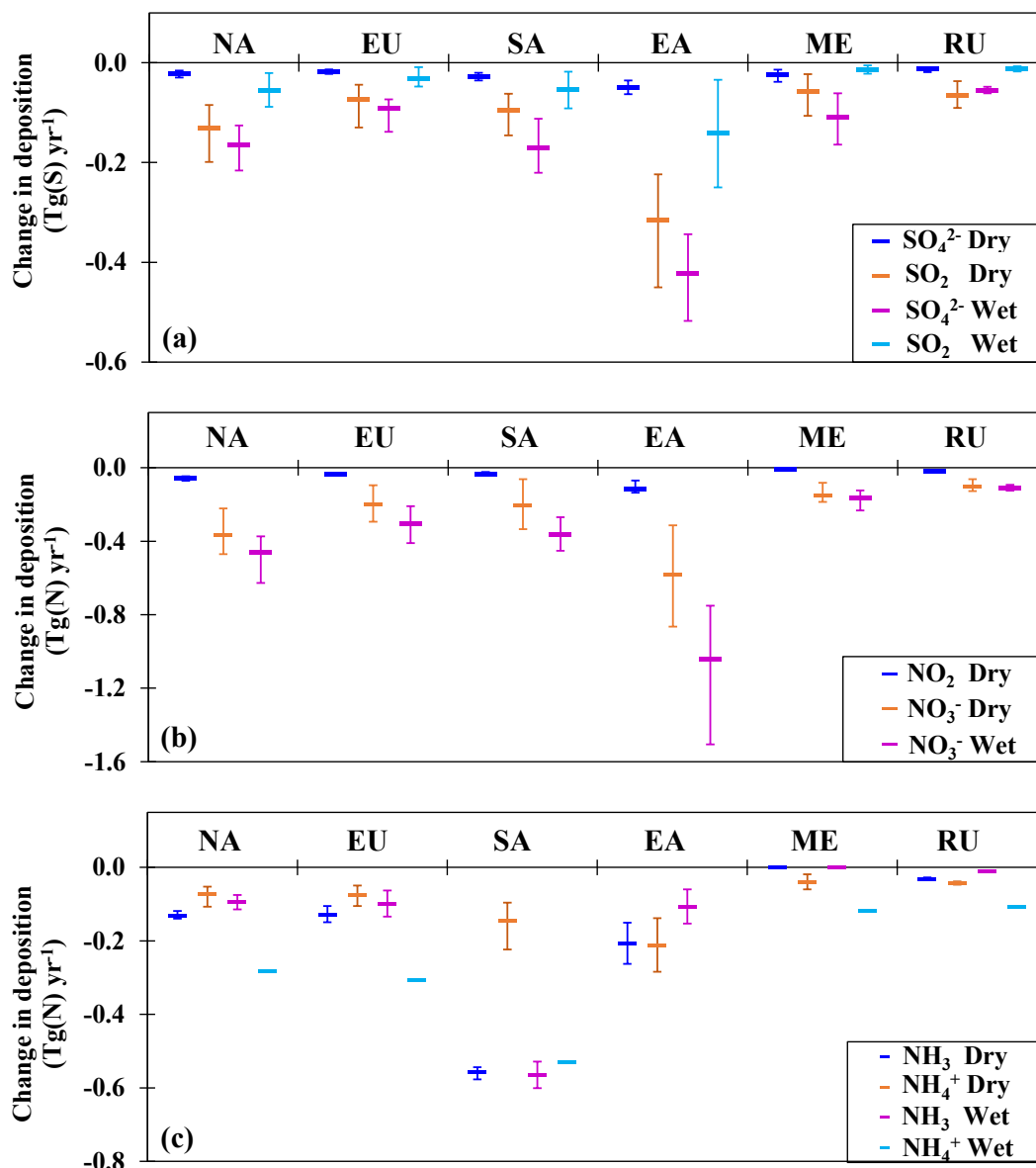


797
 798 Fig. 6 Own region and foreign contributions on own region deposition. The values are calculated
 799 by changes with 20% emission reduction. Other (OTH, pattern fill) is the contribution by other
 800 reasons than emission reduction in the 6 regions (see text for details).

801



802 Fig. 7



803
 804 Fig. 7 Inter-model variations in wet and dry deposition changes (unit: $\text{Tg(S or N) yr}^{-1}$) under
 805 emission perturbation experiments. The values are global integrated changes in components of S
 806 and N deposition for perturbation experiments from MMM results with error bars showing the
 807 max and min values among all models.
 808



809 Tables

810 Table 1. Source-receptor relationship of S/NO_y/NH_x deposition (%) for regions (including
 811 continental coastal and non-coastal regions). The values in the parentheses are for coastal regions
 812 as a subset of the total.

	Receptor Regions	Source Regions					
		NA	EU	SA	EA	ME	RU
S Deposition	NA	68.9 (8.9)	0.2 (0.1)	0.2 (0.0)	1.5 (0.6)	0.3 (0.1)	1.2 (0.6)
	EU	1.1 (0.6)	60.4 (14.4)	0.0 (0.0)	0.2 (0.1)	2.1 (0.2)	6.9 (2.5)
	SA	0.5 (0.1)	1.2 (0.3)	66.4 (10.0)	0.9 (0.4)	7.9 (1.6)	0.3 (0.1)
	EA	0.6 (0.2)	1.8 (0.4)	8.8 (1.3)	73.4 (11.5)	4.6 (0.8)	5.2 (1.4)
	ME	0.0 (0.0)	2.6 (0.6)	0.6 (0.3)	0.0 (0.0)	42.4 (8.2)	0.8 (0.2)
	RU	0.4 (0.1)	13.6 (2.2)	0.1 (0.1)	5.1 (2.2)	5.0 (1.1)	62.2 (4.4)
	Others	28.5	20.1	23.8	19.1	37.7	23.4
NO _y Deposition	NA	71.5 (7.8)	0.8 (0.2)	0.5 (0.1)	1.0 (0.3)	0.5 (0.1)	1.0 (0.3)
	EU	1.3 (0.6)	66.2 (17.5)	0.2 (0.1)	0.3 (0.1)	3.5 (0.9)	9.8 (2.9)
	SA	0.2 (0.0)	0.2 (0.0)	66.2 (8.6)	0.5 (0.2)	7.9 (1.3)	0.2 (0.0)
	EA	0.6 (0.1)	1.2 (0.2)	6.2 (0.7)	74.4 (14.3)	2.4 (0.3)	4.3 (0.9)
	ME	0.4 (0.1)	1.6 (0.3)	0.9 (0.4)	0.1 (0.0)	54.4 (8.0)	0.8 (0.2)
	RU	0.6 (0.1)	10.3 (1.3)	0.1 (0.0)	5.1 (2.2)	4.9 (1.3)	61.4 (3.1)
	Others	25.6	19.7	25.8	18.6	26.4	22.5
NH _x Deposition	NA	88.4 (5.6)	0.2 (0.1)	0.3 (0.1)	-*	0.7 (0.3)	0.4 (0.2)
	EU	0.6 (0.3)	83.2 (17.8)	0.0 (0.0)	-	4.6 (1.2)	11.9 (3.1)
	SA	0.0 (0.0)	0.1 (0.0)	85.1 (7.6)	-	8.6 (2.4)	0.0 (0.0)
	EA	0.0 (0.0)	0.4 (0.1)	4.2 (0.3)	-	2.6 (0.5)	3.8 (1.0)
	ME	0.1 (0.0)	1.3 (0.3)	0.4 (0.2)	-	49.4 (5.9)	1.5 (0.4)
	RU	0.4 (0.1)	10.3 (1.3)	0.1 (0.0)	-	7.3 (1.5)	76.9 (4.1)
	Others	10.5	4.4	9.7	-	26.9	5.7

813 * Lack of NH₄⁺ wet deposition under EA emission perturbation experiment from all models.

814

815 Table 2. RERER values of S/NO_y/NH_x deposition for continent non-coastal and coastal regions.

816 Total column gives the RERER for coastal and non-coastal together.

Regions	S deposition			NO _y deposition			NH _x deposition		
	Total	Non-coastal	Coastal	Total	Non-coastal	Coastal	Total	Non-coastal	Coastal
NA	0.17	0.12	0.40	0.17	0.12	0.43	0.07	0.05	0.31
EU	0.36	0.27	0.53	0.34	0.27	0.48	0.12	0.09	0.22
SA	0.18	0.14	0.35	0.17	0.12	0.37	0.04	0.03	0.17
EA	0.16	0.14	0.28	0.16	0.12	0.27	-	-	-
ME	0.32	0.27	0.46	0.32	0.27	0.50	0.42	0.36	0.67
RU	0.61	0.56	0.84	0.59	0.52	0.90	0.55	0.49	0.85

817